ASEAN Journal of Science and Engineering

Journal homepage: http://ejournal.upi.edu/index.php/AJSE/

Valorization of Imidazolium-Based Salts as Next-Generation Antimicrobials: Integrated Biological Evaluation, ADMET, Molecular Docking, and Dynamics Studies

Chaimae Merimi[1], Abdessamad Benabbou[1], Elmehdi Fraj[1], Oussama Khibech[1], Meryem Idrissi Yahyaoui[1], Abdeslam Asehraou[1], Mousslim Messali[2], Mohamed Anouar Harrad[3], Allal Challioui[1], Boufelja Bouammali[1], Rachid Touzani[1,], Belkheir Hammouti[4], Saud M. Almutairi[5]*

[1]University Mohammed Premier, Oujda, Morocco
[2]Imam Mohammad Ibn Saud Islamic University, Riyadh, Saudi Arabia
[3]Sultan Moulay Slimane University, Beni-Mellal, Morocco
[4]Euromed University of Fes, Fez, Morocco
[5]King Abdulaziz City for Science and Technology, Riyadh, Saudi Arabia
[*]Correspondence: E-mail: r.touzani@ump.ac.ma

ABSTRACT

This study aimed to investigate the antimicrobial potential of four imidazolium-based salt derivatives (A1–A4) using an integrated approach that combined in vitro biological assays with computational analysis. The compounds were screened against various Gram-positive and Gram-negative bacteria, as well as fungal strains, while computational methods like ADMET predictions and molecular simulations assessed their viability and mechanism. The results revealed that compounds A3 and A4 possess potent antibacterial activity comparable to gentamicin, particularly against *E. coli*, with A3 also showing significant antifungal efficacy. These findings were strongly supported by computational analysis, which predicted favorable oral bioavailability, acceptable toxicity, and confirmed a stable binding interaction with the bacterial enzyme DNA gyrase. The primary implication is the identification of A3 and A4 as promising therapeutic candidates for developing new antimicrobials to combat drug-resistant pathogens, validating this integrated research strategy for future drug discovery.

ARTICLE INFO

Article History:
Submitted/Received 25 May 2025
First Revised 27 Jun 2025
Accepted 28 Aug 2025
First Available online 29 Aug 2025
Publication Date 01 Mar 2026

Keyword:
ADMET,
Antimicrobial activity,
Imidazolium salts,
Molecular docking,
Molecular dynamics.

1. INTRODUCTION

Imidazolium-based salts [1, 2] have emerged as a focal point in medicinal chemistry [3] due to their diverse biological activities [4, 5], particularly their antifungal [6] and antibacterial properties [7]. Renowned for their structural versatility, chemical stability, and ability to interact with biological targets [8], these compounds hold significant promise for pharmaceutical applications [9, 10]. In recent years, the escalating threat of drug-resistant microbial [11] infections has become a pressing global health crisis, highlighting the urgent need for innovative antimicrobial agents that are effective, environmentally sustainable, and safe for long-term use [12]. This research aligns with global sustainability objectives by addressing the environmental and public health challenges posed by drug-resistant pathogens, while promoting the development of eco-friendly therapeutic solutions. In this study, six previously synthesized imidazole-based salts were rigorously evaluated for their antimicrobial potential [13, 14] against a panel of Gram-positive bacteria [15] (Staphylococcus aureus and Micrococcus luteus) and Gram-negative bacteria [16] (Escherichia coli and Pseudomonas aeruginosa). Additionally, their antifungal activity was assessed against four fungal strains: Candida glabrata, Rhodotorula glutinis, Aspergillus niger, and Penicillium digitatum [17]. These pathogens are known to cause severe infections, particularly in immunocompromised individuals, and exhibit increasing resistance to conventional antibiotics and antifungal agents. By targeting these resistant strains, this research contributes to sustainable healthcare strategies, aiming to reduce the overuse of existing treatments and minimize their environmental impact.

To further support the development of these compounds, a molecular docking study [18, 19] was carried out to investigate their potential interaction with Escherichia coli DNA gyrase [20], a validated antibacterial target. DNA gyrase is essential for bacterial DNA replication and transcription, making it a prime target for drug development. The docking study revealed strong binding affinities between the synthesized salts and the enzyme's active site, suggesting their potential as effective bacterial inhibitors. Redocking of the reference inhibitor Clorobiocin confirmed the reliability of the docking protocol, with an RMSD value of 1.05 Å. Additionally, an in-silico Absorption, Distribution, Metabolism, Excretion, and Toxicity (ADMET) analysis was conducted to predict their pharmacokinetic behavior and toxicity profiles [21-23]. Key parameters were evaluated to assess their drug-likeness and safety [24], including solubility, lipophilicity, intestinal absorption, metabolic stability, clearance, and toxicity risks. This computational approach not only streamlines the drug discovery process but also aligns with sustainable practices by reducing the need for extensive laboratory testing, conserving resources, and optimizing material use. A thorough understanding of these properties is essential for guiding structural modifications that enhance efficacy while ensuring biocompatibility and environmental safety [25].

This study seeks to advance the valorization of imidazolium-based salts as next-generation antimicrobial agents by integrating biological evaluations with in silico ADMET predictions. The results offer valuable insights into their mechanisms of action, pharmacokinetic behavior, and potential limitations, thereby laying a solid foundation for their further development as effective and sustainable therapeutic candidates. By addressing both therapeutic efficacy and environmental impact, this research aligns with long-term strategies to combat antimicrobial resistance and promote eco-conscious pharmaceutical innovation. Ultimately, the study contributes to global health advancement and environmental preservation, offering a viable pathway toward more resilient and sustainable healthcare systems.

DOI: https://doi.org/10.17509/ajse.v6i1.89789
p- ISSN 2776-6098 e- ISSN 2776-5938

2. METHODS

2.1. Synthesis of Salts

The four imidazole-based salts utilized in this study were synthesized using a methodology previously detailed in our anti-corrosion research (**Figure 1**) [26]. The synthesis process involved the N-alkylation of imidazole derivatives with suitable alkyl halides in the presence of a base catalyst, resulting in the formation of imidazolium salts. The reaction was conducted under reflux conditions in polar solvents to optimize yield and purity. Following the reaction, the crude products were purified using recrystallization or column chromatography, and their structural integrity was confirmed through spectroscopic techniques, including NMR and FTIR analysis. Initially investigated for their corrosion inhibition capabilities, these salts are now being repurposed and valorized for their antimicrobial potential. This transition underscores their versatility and aligns with sustainable practices by extending the utility of existing compounds. Through comprehensive biological screening and computational ADMET analysis, this study aims to unlock their therapeutic potential, contributing to the development of novel antimicrobial agents while promoting resource efficiency and long-term material management.

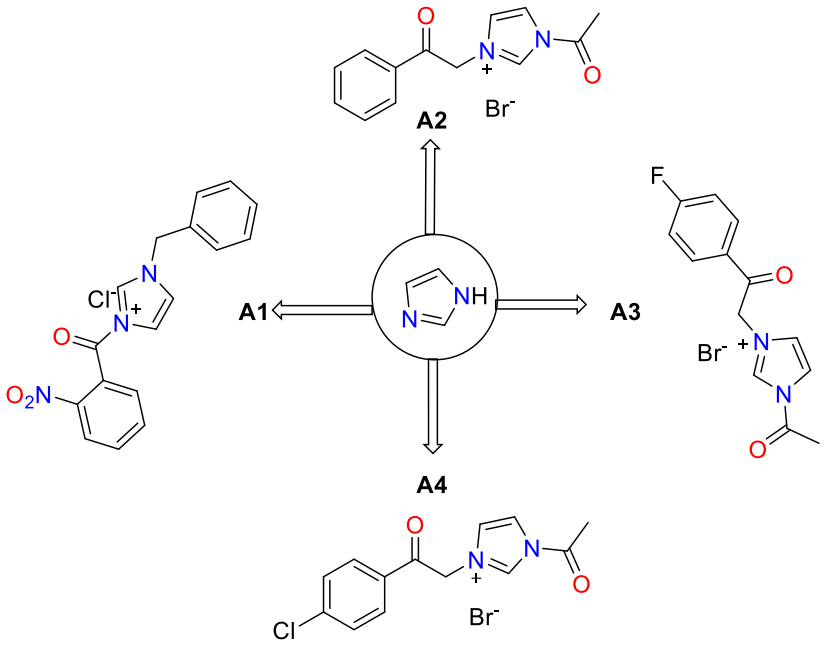

Figure 1. General procedure of synthesis of imidazolium salts.

2.2. Antibacterial Studies

We examined antibacterial efficacy against two Gram-positive strains, Staphylococcus aureus ATCC 6538P and Micrococcus luteus LB 14110, and two Gram-negative strains, Pseudomonas aeruginosa ATCC 15442 and Escherichia coli ATCC 10536. Antifungal effectiveness was measured against Candida glabrata, Rhodotorula glutinis ON 209167, Aspergillus niger, and Penicillium digitatum. To find the MIC, we tested concentrations from 16 to 0.125%. The method involved 96-well microplates and the broth microdilution process. To each well, we added 50 µL of the microbial inocula standardized to 105 cells/mL. Positive controls matched the microorganism's tetracycline for bacteria and cycloheximide for fungi [27]. The plates incubated at 37°C for 24 hours for bacteria, and at 25°C for 48 hours for fungi, were later augmented with 15 µL of 0.015% resazurin and incubated further for 2 hours to

DOI: https://doi.org/10.17509/ajse.v6i1.89789
p- ISSN 2775-6793 e- ISSN 2775-6815

check metabolic activity. A change from blue resazurin to pink resorufin indicated viability. Each test was conducted in triplicate for precision.

2.3. Antifungal Activities

The antifungal activities of diazole derivatives were evaluated using the agar well diffusion method. The fungal strains used were Candida albicans ATCC 10231, Aspergillus niger ATCC 16404, and Trichophyton mentagrophytes ATCC 9533. The diazole derivatives were dissolved in dimethyl sulfoxide (DMSO) to obtain solutions at concentrations of 10, 50, and 100 µg/mL. The fungal strains were cultured on Sabouraud agar plates, and spore suspensions (106 spores/ml) were spread on the surface of the plates. Wells of 6 mm in diameter were created in the agar and filled with 100 µL of each diazole derivative solution. The plates were incubated at 28°C for 48 hours. Antifungal activity was determined by measuring the diameter of the inhibition zone around the wells. Fluconazole was used as a positive control, and DMSO was used as a negative control [27-29]. The results were analysed by comparing the inhibition zones obtained with those of the controls.

2.4. ADMET Studies

2.4.1. Pharmacokinetic Analysis Using Computational Tools

A compound's pharmacokinetic profile, encompassing absorption, distribution, metabolism, and excretion (ADME), arises from a series of biochemical and physiological interactions that determine its behavior in biological systems. A thorough understanding of these parameters clarifies how compounds are absorbed, systemically distributed, metabolized, and ultimately eliminated. In recent years, computational approaches have gained prominence for analyzing and predicting ADME properties, leveraging in silico simulations of membrane permeability, biomolecular interactions during absorption and excretion, and structural stability throughout the metabolic process [30]. In this study, the molecular structures of the target compounds were initially drawn in ChemDraw, and their SMILES notations were extracted for further computational evaluation. These SMILES strings were then processed using two key prediction platforms: SwissADME and pkCSM [31, 32].

Both tools provided robust models for forecasting pharmacokinetic parameters, offering comprehensive insights into each compound's potential pharmacological behavior (e.g., absorption, tissue distribution, metabolic pathways) under physiologically relevant conditions, as well as toxicity risk assessments. By integrating predictions from SwissADME and pkCSM, it was possible to refine the overall interpretation of how each compound might perform in vivo, thus laying a rational foundation for subsequent experimental validation.

2.4.2. Prediction of the Toxicity Analysis (Pro Tox III)

Prospective toxicity evaluations were performed using the ProTox-III online platform, following established guidelines [33]. This platform processes chemical structures input as SMILES strings, employing advanced statistical models and machine learning algorithms. The SMILES codes, generated in ChemDraw, were validated and cross-referenced with an extensive toxicological database, yielding detailed information on each compound's structural and chemical features. By providing estimated LD_{50} values for acute toxicity and GHS classification data, ProTox-III offers a comprehensive perspective on potential toxicological endpoints. This structured toxicity assessment facilitates the judicious selection of promising molecules for subsequent in vivo validation. In addition, the platform's speed and precision in toxicity analysis support data-driven decision-making in both pharmaceutical research and environmental risk management.

DOI: https://doi.org/10.17509/ajse.v6i1.89789
p- ISSN 2776-6098 e- ISSN 2776-5938

2.5. PyRx: Preparation, Configuration, and Validation of the Docking Protocol

Docking simulations were carried out using PyRx, which integrates AutoDock Vina with the AutoDock Tools (ADT) interface (version 1.5.7) [34]. Before docking, the receptor (*.pdbqt) files were prepared by removing crystallographic water molecules, adding polar hydrogens, and assigning charges according to the AutoDock suite's guidelines. Any additional protein preprocessing (e.g., deleting superfluous water, correcting structural issues) was handled in Discovery Studio, which was also used to visualize the resulting poses and analyze ligand–receptor interactions post-docking. Each ligand was initially drawn and optimized in ChemDraw, then subjected to energy minimization. The final ligand structures were converted into PDBQT format via ADT (version 1.5.7), ensuring proper geometric and electronic configurations for docking. For the 1KZN receptor, the search space was defined by a bounding box centered at (x = 18.62, y = 30.58, z = 36.61) with dimensions (12.7 × 15.88 × 16.24), and the exhaustiveness parameter was set to 8. As part of protocol validation, the co-crystallized ligand for 1KZN was re-docked into its active site, yielding an RMSD of 0.234 Å relative to its experimental conformation. This value is well below the conventional threshold of 2 Å, confirming the reliability and robustness of the chosen docking procedure for 1KZN. For the three additional protein targets (1U1Z, 1JIJ, and 6KQ9), a blind docking approach was employed, wherein the entire protein surface was considered as the potential binding site rather than specifying a predefined box. Under these conditions, AutoDock Vina's scoring function was again used to rank the resulting poses, maintaining the same exhaustiveness level (8) and default parameters for all simulations.

2.6. Implementation of Molecular Dynamics Simulations Using GROMACS

The protein file (P.pdb) was prepared using the gmx pdb2gmx command under the AMBER99SB-ILDN force field, ensuring missing hydrogen atoms were added and protonation states assigned automatically. The ligand (LIG.pdb) was subsequently parameterized, and the resulting .gro and .itp files were verified. A protein-ligand complex (complex.pdb) was then created by merging the parameterized ligand with the protein, placed in a cubic simulation box, solvated with the TIP3P water model, and neutralized by adding the required ions. After standard GROMACS [35] energy minimization and equilibration procedures, a production simulation was conducted with periodic recording of atomic coordinates and velocities. This workflow allowed the evaluation of the complex's stability, structural dynamics, and key interactions under conditions closely resembling physiological environments.

3. RESULTS AND DISCUSSION

3.1. Antibacterial activities

The evaluation of the ligands was conducted with Gram-positive bacteria Staphylococcus aureus and Micrococcus luteus, and two Gram-negative bacteria, Escherichia coli and Pseudomonas aeruginosa. The results are shown in **Figure 2**. In this study, four heterocyclic ligands were evaluated for their antimicrobial activity against four bacterial strains, comprising both Gram-positive and Gram-negative bacteria. The Gram-positive bacteria tested were Staphylococcus aureus and Micrococcus luteus, while the Gram-negative bacteria included Escherichia coli and Pseudomonas aeruginosa. Two ligands, A3 and A4, showed significant inhibition results against these bacterial strains, indicating promising antibacterial potential (**Table 1**). Ligand A3 demonstrated strong activity against Escherichia coli, with an inhibition zone of 31 mm, comparable to the positive control Gentamicin (T+),

DOI: https://doi.org/10.17509/ajse.v6i1.89789
p- ISSN 2775-6793 e- ISSN 2775-6815

which showed 31.01 mm inhibition. A3 also inhibited Pseudomonas aeruginosa with a 28 mm inhibition zone, closely approaching the T+ result of 33.5 mm.

Ligand Sm48 exhibited broad-spectrum efficacy across both Gram-positive and Gram-negative bacteria. It showed inhibition zones of 22 mm against Staphylococcus aureus and Micrococcus luteus, compared to 32.7 mm and 30.66 mm with T+, respectively. For Gram-negative bacteria, Sm48 produced inhibition zones of 28 mm against Escherichia coli and 25 mm against Pseudomonas aeruginosa, which were also comparable to T+ values of 31.01 mm and 33.5 mm, respectively. These results highlight the potential of ligands A3 and A4 as effective antimicrobial agents, particularly against both Gram-positive and Gram-negative bacterial strains.

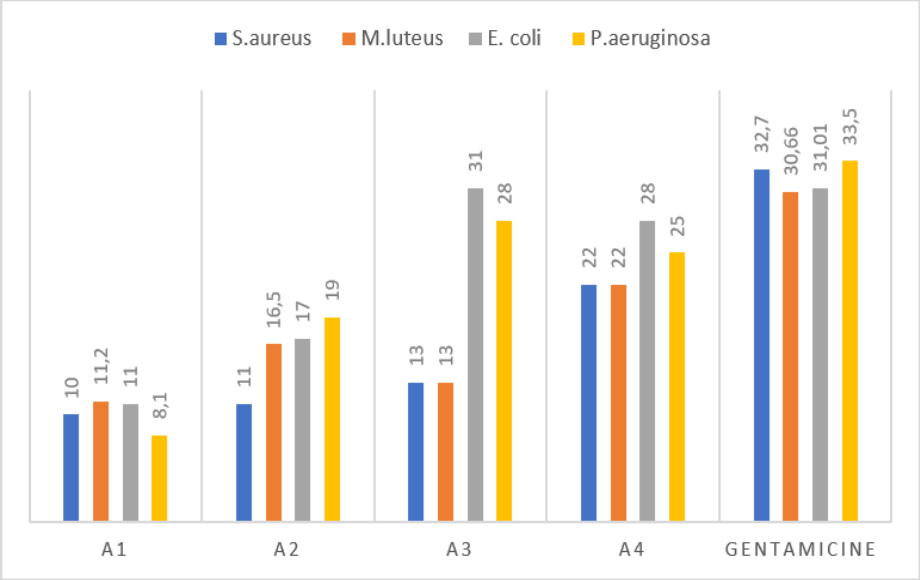

Figure 2. Antibacterial Activity of imidazolium salts.

Table 1. Antibacterial activity "inhibition zone in mm".

	Staphylococcus aureus	***Micrococcus luteus***	***Escherichia coli***	***Pseudomonas aeruginosa***
	Inhibition Zone (mm)			
A1	10±0.2	11.2±0.1	11±0.1	8.1±0.2
A2	11±0.1	16.5±0.2	17±0.2	19±0.1
A3	13±0.3	13±0.4	31±0.2	28±0.1
A4	22±0.1	22±0.2	28±0.1	25±0.1
T- DMSO	ND	ND	ND	ND
T+ Gentamicine	32.7±0.1	30.66±0.1	31.01±0.9	33.5±0.7

The tests showed that the diazole derivatives, particularly A3 and A4, exhibited significant antibacterial activity against both Gram-positive (Staphylococcus aureus and Micrococcus luteus) and Gram-negative bacteria (Pseudomonas aeruginosa and Escherichia coli) (**Table 2**). Specifically, A3 demonstrated comparable inhibition to the positive control (gentamicin), with inhibition zones of 31 mm against E. coli and 28 mm against P. aeruginosa, showing impressive antibacterial efficacy. These results suggest that these derivatives could be used as antimicrobial agents in the treatment of infections resistant to conventional antibiotics, a growing public health concern.

DOI: https://doi.org/10.17509/ajse.v6i1.89789
p- ISSN 2776-6098 e- ISSN 2776-5938

Table 2. Growth inhibition effectiveness of compound salts using MIC and MBC.

	Staphylococcus aureus		*Micrococcus luteus*		*Escherichia coli*		*Pseudomonas aeruginosa*	
	MIC	**MBC**	**MIC**	**MBC**	**MIC**	**MBC**	**MIC**	**MBC**
A1	-	-	-	-	-	-	-	-
A2	-	-	6.66	> 13.33	6.66	> 13.33	3.33	13.33
A3	> 13.33	> 13.33	> 13.33	> 13.3	0.20	0.83	0.20	6.66
A4	0.83	3.33	0.83	3.33	0.20	0.83	0.41	1.66

T+: Tetracycline (1mg/mL) for antibacterial activity.

3.2. Antifungal Activities

In our antifungal screening, four heterocyclic ligands were evaluated against four fungal strains: Candida glabrata, Rhodotorula glutinis (ON 209167), Aspergillus niger, and Penicillium digitatum. Among the tested ligands, A3 displayed the most promising antifungal activity, showing comparable inhibition to the positive control, Cycloheximide (T+), against all four strains. The results are shown in **Figure 3** and **Table 3**.

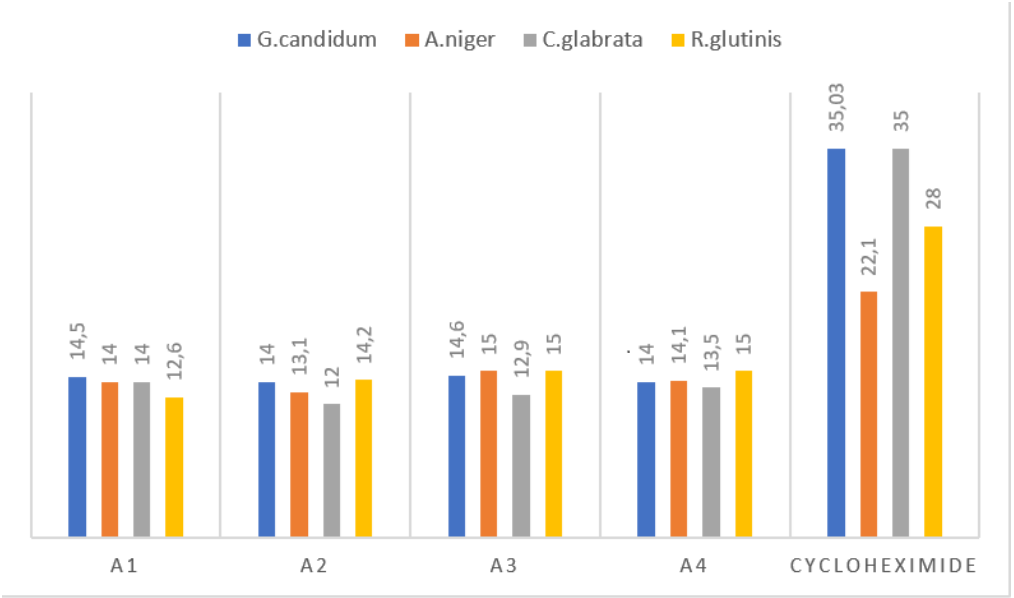

Figure 3. Antifungal activity of imidazolium salts.

Specifically, A3 achieved an inhibition zone of 14.6 mm against Candida glabrata, close to the T+ inhibition of 35.05 mm. For Rhodotorula glutinis (ON 209167), A3 recorded a 15 mm inhibition zone, comparable to the T+ inhibition of 22.1 mm. Against Aspergillus niger, SM47 produced an inhibition zone of 12.9 mm, approaching the T+ result of 35 mm. Lastly, SM47 showed a 15 mm inhibition against Penicillium digitatum, while the T+ control achieved 28 mm. These findings suggest that ligand A3 has noteworthy antifungal properties and potential as a broad-spectrum antifungal agent, given its efficacy across both yeast and mold strains, despite the naturally higher inhibition values observed with Cycloheximide. Regarding antifungal activity, A3 proved particularly promising, showing inhibition zones that were comparable to positive controls against several fungal strains, including Candida glabrata, Rhodotorula glutinis, Aspergillus niger, and Penicillium digitatum. Although the inhibition values were naturally higher with the control (cycloheximide), A3 still demonstrated considerable antifungal activity. These findings suggest that A3 has broad-spectrum

DOI: https://doi.org/10.17509/ajse.v6i1.89789
p- ISSN 2775-6793 e- ISSN 2775-6815

antifungal properties, making it a potential candidate for treating both yeast and mold infections (**Table 4**).

Table 3. Antifungal activity "inhibition zone in mm".

	Geotrichum candidum	***Aspergillus niger***	***Candida glabrata***	***Rhodotorula. glutinis***
	Inhibition Zone (mm)			
A1	14.5±0.2	14±0.2	14±0.2	12.6±0.2
A2	14±0.1	13.1±0.1	12±0.1	14.2±0.2
A3	14.6±0.3	15±0.2	12.9±0.3	15±0.3
A4	14±0.3	14.1±0.2	13.5±0.4	15±0.1
T- DMSO	ND	ND	ND	ND
T+	35.03±0.2	22.1±0.1	35.02±0.1	28.01±0.1

Table 4. Growth inhibition effectiveness of compound salts using MIC and MBC.

	Geotrichum candidum		***Aspergillus niger***		***Candida glabrata***		***Rhodotorula. Glutinis***	
	MIC	**MFC**	**MIC**	**MFC**	**MIC**	**MFC**	**MIC**	**MFC**
A1	13.33	>13.33	13.33	>13.33	13.33	>13.33	>13.33	>13.33
A3	13.33	>13.33	>13.33	>13.33	>13.33	>13.33	13.33	>13.33
A3	13.33	>13.33	13.33	>13.33	>13.33	>13.33	13.33	>13.33
A4	13.33	>13.33	13.33	>13.33	>13.33	>13.33	13.33	>13.33

T+: Cycloheximide (1 mg/mL) for antifungal activity

3.3. ADMET results

3.3.1. Comparative Analysis of Imidazolium Derivatives vs. Ciprofloxacin (Physicochemical & PK)

Before turning attention to the findings in **Table 5**, it bears emphasizing why ciprofloxacin was adopted as the standard. Esteemed among fluoroquinolones, ciprofloxacin possesses formidable antibacterial properties and a thoroughly documented pharmacokinetic background, making it a prime choice for assessing emerging imidazolium-based compounds. Although initial experimentation touched on antifungal inquiries, the main thrust of the insilico evaluations is on antibacterial performance, an arena in which ciprofloxacin has historically achieved remarkably positive results [36]. When ciprofloxacin (M5) is contrasted with the four newer entities (A1, A2, A3, A4), one can observe that all five specimens fit into a positive physicochemical spectrum that correlates with "drug-likeness." This evaluation draws on factors such as molecular weight, topological polar surface area (TPSA), hydrogen-bonding capacity, lipophilicity (CLogP), and structural flexibility. Specifically, ciprofloxacin (331.34 g/mol) has the largest molecular weight, whereas A2 (229.25 g/mol) registers the smallest, followed in ascending order by A3 (247.24 g/mol) and A4 (263.70 g/mol). A1 (308.31 g/mol) stands closer to ciprofloxacin in terms of complexity and prospective distribution. As for hydrogen-bond donors, ciprofloxacin possesses two, which could favor solubility but occasionally inhibit passive membrane diffusion; in contrast, A1-A4 have none (0). In the same vein, ciprofloxacin (TPSA = 74.57 Å²) and A1 (TPSA = 71.7 Å²) reveal significantly larger polar surface areas than A2, A3, and A4 (circa 43 Å²), suggesting reduced overall polarity for the latter trio. Ciprofloxacin also surpasses A1-A4 in the number of

DOI: https://doi.org/10.17509/ajse.v6i1.89789
p- ISSN 2776-6098 e- ISSN 2776-5938

hydrogen-bond acceptors (five compared to two or three), reflecting inherent structural discrepancies between the quinolone scaffold and imidazolium frameworks. Despite a variation in rotatable bond counts (ranging from three for ciprofloxacin to five for A1), none of these molecules violate Lipinski's or Veber's guidelines, which bolsters the case for their oral bioavailability [37, 38]. The CLogP values for A1-A4 (0.76-1.34) and ciprofloxacin (1.1) indicate a moderate level of lipophilicity, favoring a beneficial balance between water solubility and membrane traversal, consistent with a predicted high gastrointestinal uptake across all five candidates. Moreover, an identical bioavailability score (0.55) implies that, from an insilico viewpoint, A1-A4 might display pharmacokinetic behavior akin to ciprofloxacin. All these points converge to demonstrate a pronounced structural and pharmaceutical compatibility between the imidazolium-based derivatives and the reference antibiotic, underscoring the need for further in vivo studies. Such studies will ultimately confirm their genuine therapeutic promise, safety aspects, and practical bioavailability when compared directly against this well-recognized clinical agent.

Table 5. Comparison of physicochemical parameters and "Drug-likeness" profiles between ciprofloxacin (M5) and imidazolium-based derivatives (A1-A4).

Molecules	A1	A2	A3	A4	Ciprofloxacin
Molecular WEIGHT(g/mol)	308.31	229.25	247.24	263.7	331.34
H-bond acceptors	3	2	3	2	5
H-bond donors	0	0	0	0	2
Rotatable bonds	5	4	4	4	3
TPSA (Å²)	71.7	42.95	42.95	42.95	74.57
CLogP	1.34	0.76	1	1.2	1.1
GI absorption	High	High	High	High	High
Lipinski: violations	0	0	0	0	0
Veber: violations	0	0	0	0	0
Bioavailability Score	0.55	0.55	0.55	0.55	0.55

3.3.2. Influence Des Substituants Sur l'Activité Métabolique Et l'inhibition Des CYP450

These ADMETlab3 predictions (**Table 6)** highlight how subtle variations in the chemical scaffolds of the imidazolium-based derivatives (A1-A4) translate into different propensities for interacting with cytochrome P450 enzymes, specifically CYP2D6 and CYP3A4, in both inhibitory (inh) and substrate (sub) capacities [39]. At one end of the spectrum, ciprofloxacin exhibits extremely low predicted values for inhibition of CYP2D6 and CYP3A4 (on the order of 10-8 to 10-9), reflecting its rigid bicyclic quinolone structure, which limits the molecule's capacity to bind and modulate these enzymes' active sites. In contrast, the four imidazolium derivatives display more pronounced numerical values (from 0.01 up to ~0.8 for inhibition probabilities and ~0.13 for substrate scores in some cases), signifying a higher likelihood of interfering with or being metabolized by these enzymes.

Table 6. ADMETlab3 predictions (CYP2D6/CYP3A4 inhibition/substrate) for imidazolium derivatives (A1-A4) vs. ciprofloxacin.

Molecules	A1	A2	A3	A4	Ciprofloxacin
CYP2D6-inh	0.01	0.4	0.73	0.817	5.54×10^{-8}
CYP2D6-sub	0.0262	0.014819	0.129	0.015	1.072×10^{-8}
CYP3A4-inh	0.0451	5.98×10^{-7}	1.38×10^{-5}	7.5×10^{-6}	4.57×10^{-9}
CYP3A4-sub	0.014	9.21×10^{-7}	2.8×10^{-7}	4.99×10^{-7}	0.023

DOI: https://doi.org/10.17509/ajse.v6i1.89789
p- ISSN 2775-6793 e- ISSN 2775-6815

From a structural standpoint, the imidazolium core in A1-A4 is more flexible and carries different substituents (e.g., nitro, halogen, or benzyl-acetyl moieties) that can engage in hydrogen-bonding, π-π interactions, or dipolar contacts within the enzymes' binding pockets. A1, for instance, with moderate to low numerical values in both inhibition and substrate columns (e.g., 0.01 and 0.0262 for CYP2D6), may have a conformation that partially fits into the CYP2D6 active site enough to be recognized but not so extensively that it becomes a potent inhibitor.

Meanwhile, A2's higher CYP2D6-inh value (0.4) can be rationalized by a substituent pattern that aligns more strongly with the hydrophobic and aromatic residues in the CYP2D6 binding region, thereby increasing inhibitory potential. A3 and A4, containing halogen-substituted phenyl rings, each display exceptionally low predicted values for 3A4-inh (e.g., 1.38824×10^{-5} and 7.5×10^{-6}), suggesting that the spatial orientation or electronic distribution of their halogen groups may hinder stable binding to the CYP3A4 catalytic site, reducing inhibition likelihood despite the possibility of partial substrate recognition (reflected by smaller but non-negligible "sub" values). Overall, these results underscore the powerful role of structure-activity relationships in drug metabolism: even modest differences in side-chain substitution (nitro vs. halogen vs. acetyl) or ring connectivity (as in ciprofloxacin's fused quinolone system) markedly alter how each compound might interfere with or be processed by CYP2D6 and CYP3A4. The consistent theme is that ciprofloxacin's more rigid, bicyclic framework and well-known polar contacts confer a distinct ADME profile with minimal enzyme modulation, whereas the imidazolium derivatives, owing to their charged core and variable substituents, show broader spectrums of predicted substrate or inhibitor behavior, aligning closely with their structural diversity.

3.3.3. Comparative Analysis of Thermal Properties and Metabolic Stability (SPR)

Figure 4 reveals notable variations in melting point (mp), boiling point (bp), and half-life (t0.5, in minutes) among the imidazolium derivatives (A1, A2, A3, A4) and ciprofloxacin, illustrating the direct influence of their chemical structures on physicochemical properties and stability [40]. First, the marked increase in melting point seen in A3 (129 °C) and A4 (120 °C), compared with A1 (77 °C) and A2 (93 °C), reflects stronger intermolecular interactions (hydrogen bonds, π-π stacking, dipolar forces) promoted by aromatic or halogen substitutions. For instance, A3 appears to form a denser crystalline network thanks to its para-halogen substituent. In contrast, the nitro or benzyl motif in A1, less suited to high symmetry, leads to a lower melting point. Ciprofloxacin (222 °C) far exceeds these derivatives owing to its bicyclic quinolone system and notable capacity for both intra- and intermolecular hydrogen bonding, which increases its enthalpy of fusion. Regarding boiling points, A1 (304 °C) and A4 (301 °C) are on par with ciprofloxacin (297 °C), indicating that polar or halogen substituents (F, Cl) can raise the vaporization temperature, while A2 (268 °C) and A3 (295 °C) show how the nature and arrangement of aromatic substituents modulate overall volatility.

The half-life (t0.5) data, expressed here in minutes, confirms greater persistence for ciprofloxacin, about 92 minutes, likely stemming from its rigid, sterically hindered structure that reduces potential sites for hydrolysis or oxidation. Meanwhile, the imidazolium derivatives A1-A4 range from roughly 24 minutes (0.40 hours) to about 54 minutes (0.895 hours), reflecting a heightened susceptibility to degradation, probably due to fewer stabilizing intramolecular interactions and greater exposure to enzymatic processes. Overall, these melting point, boiling point, and half-life differences underscore a clear structure-property relationship (SPR): the nature and positioning of substituents (nitro, halogen, acetyl), the rigidity or flexibility of the molecular skeleton, and the presence of polar sites collectively govern solid-state cohesion, thermal stability, and metabolic resilience for each compound.

DOI: https://doi.org/10.17509/ajse.v6i1.89789
p- ISSN 2776-6098 e- ISSN 2776-5938

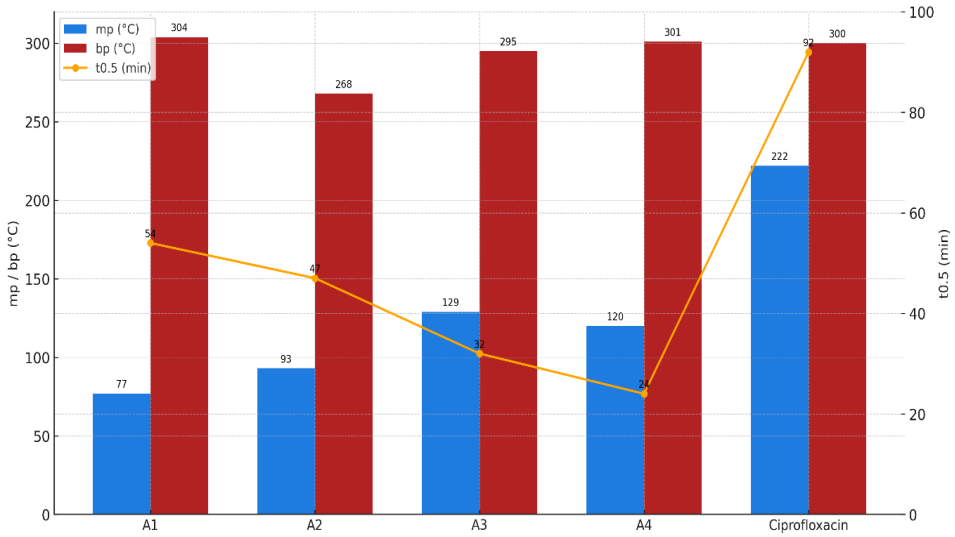

Figure 4. Comparing MP, BP, and $t_{0.5}$ for Imidazolium Derivatives vs. Ciprofloxacin (ADMETlab3).

3.3.4. Acute Toxicity Insights: Linking Structure and LD_{50} Predictions

These toxicity assessments (**Figure 5**) indicate that all imidazolium-based derivatives (A1-A4) fall under "Class 4 Toxicity," with modeled oral LD_{50} values spanning 560 mg/kg (A2, A3, A4) to 1000 mg/kg (A1). Meanwhile, ciprofloxacin, also categorized as Class 4, exhibits a considerably higher LD_{50} (2000 mg/kg) [41]. From a structural perspective, the lower figures (560-1000 mg/kg) for A1-A4 suggest a greater potential for acute toxicity compared to ciprofloxacin, attributable to multiple factors.

First, the imidazolium core imparts a permanent positive charge that can facilitate electrostatic interactions or compromise certain membranes, thus heightening systemic toxicity. Moreover, substituent type and positioning (e.g., the nitro moiety on A1, or halogenated/phenyl groups on A2-A4) affect each compound's reactivity and likelihood of producing harmful metabolites.

For instance, A1 (LD_{50} = 1000 mg/kg) possesses a nitro substituent that could trigger reduction reactions or oxidative stress, yet its overall conformation may limit absorption or tissue distribution, explaining a marginally lower toxicity than A2-A4 (560 mg/kg). In contrast, halogenated substituents (A2, A3, A4) frequently correlate with improved membrane penetration and metabolic pathways that form more toxic byproducts, thereby reducing the LD_{50} [42].

By comparison, ciprofloxacin (LD_{50} = 2000 mg/kg) features a well-characterized quinolone skeleton that is more stable and less prone to generating reactive intermediates; its rigid bicyclic design and well-arranged polar groups foster a safer toxicological profile, despite being in the same formal toxicity class.

Ultimately, these findings affirm a strong link between chemical structure and acute toxicity, emphasizing how overall charge, substituent identity, and metabolic robustness drive the observed divergences between imidazolium derivatives and ciprofloxacin.

DOI: https://doi.org/10.17509/ajse.v6i1.89789
p- ISSN 2775-6793 e- ISSN 2775-6815

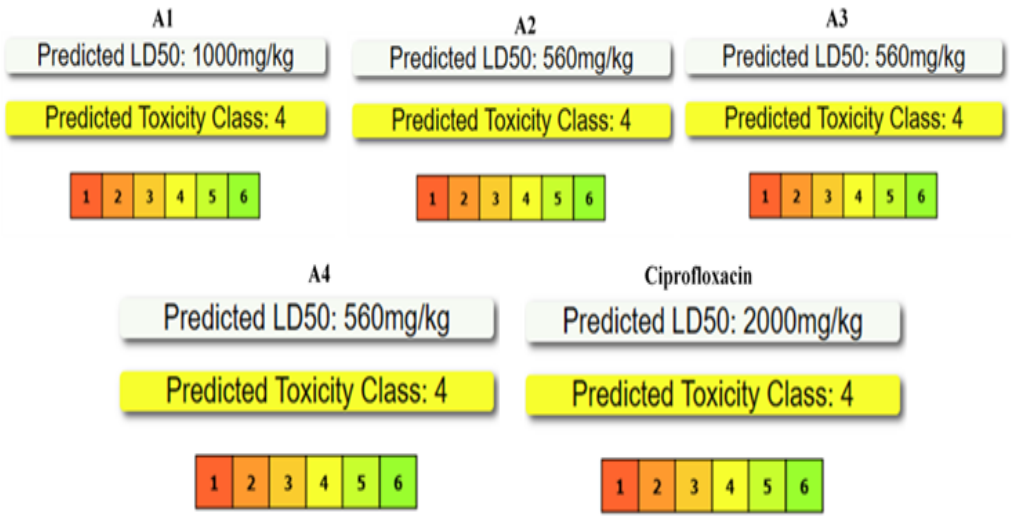

Figure 5. Predicted acute toxicity (LD_{50}) for imidazolium-based derivatives (A1-A4) versus ciprofloxacin.

3.4. Docking study

To gain additional proof and validation of the in vitro antibacterial performances we observed in our imidazolium derivatives, we targeted key bacterial enzymes bearing the PDB codes 1U1Z, 1KZN, 1JIJ, and 6KQ9 (**Figure 6**) [43-46]. These codes pinpoint vital three-dimensional protein structures at the heart of metabolic pathways in pathogenic bacteria such as Pseudomonas aeruginosa, Escherichia coli, Staphylococcus aureus, and Micrococcus luteus.

We employed ciprofloxacin, a fluoroquinolone antibiotic known for its notable antibacterial strength, as a reference molecule in the molecular docking phase, thus enabling direct comparison to our imidazolium derivatives.

Because these protein architectures are available at high resolution, we can perform a detailed and trustworthy inspection of their ligand-binding patterns. Consequently, the docking outputs will shed light on the structural framework underlying the observed in vitro biological activities, confirming the promising therapeutic relevance of imidazolium derivatives when measured against ciprofloxacin.

A closer look at the binding affinities (in kcal/mol) in **Table 7** indicates that ciprofloxacin consistently shows some of the most negative (and thus most favorable) values across the four targets. Nevertheless, certain imidazolium derivatives, particularly A1 in the docking calculations, display affinities that are on par with or occasionally surpass those of ciprofloxacin, as observed with P. aeruginosa (1U1Z). At the same time, derivatives like A3 and A4 exhibit superior activity in vitro, suggesting that while the predicted binding energies point to strong protein-ligand interactions, additional in vitro factors (e.g., cell penetration or efflux mechanisms under laboratory conditions) could also affect antibacterial efficacy.

Overall, the docking results confirm the high potential of these imidazolium derivatives and underscore ciprofloxacin's role as a robust comparator, highlighting a promising array of binding profiles within this series of compounds.

DOI: https://doi.org/10.17509/ajse.v6i1.89789
p- ISSN 2776-6098 e- ISSN 2776-5938

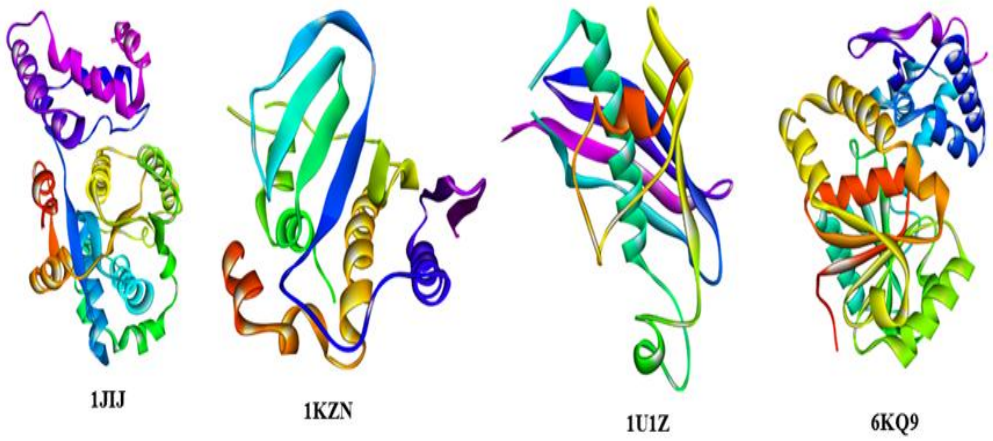

Figure 6. Three-Dimensional Visualization of the Bacterial Enzymatic Targets (PDB Codes: 1JIJ, 1KZN, 1U1Z, and 6KQ9).

Table 7. Predicted binding energies (kcal/mol) for imidazolium derivatives and ciprofloxacin against four bacterial targets.

	S. aureus	E. Coli	P. aeruginosa	M. luteus
Structure	1JIJ	1KZN	1U1Z	6KQ9
A1	-9	-7.6	-6.9	-7.9
A2	-7.5	-7	-5.9	-7.2
A3	-7.8	-7.4	-6	-7.4
A4	-7.4	-7.3	-5.8	-7.6
Ciprofloxacin	-9.4	-7.7	-6.7	-8.1

*Building affinity (kcal/mole)

Before examining **Figure 7**, it is important to note that the choice of the A4 compound for the docking simulation with the E. coli protein (PDB: 1KZN) was guided by two key considerations: on the one hand, A4 demonstrated particularly promising in vitro results; on the other, the validated docking protocol using this protein showed increased reliability in predicting interactions. The 2D interaction diagram reveals that A4 establishes a variety of non-covalent bonds with 1KZN, reflecting a favorable steric and electronic complementarity within the complex. Notably, the ligand's carbonyl oxygen forms a C-H hydrogen bond with Asn A:46 (≈3.59 Å), anchoring A4 in the binding pocket, while the halogen substituent (chlorine) on the aromatic ring creates a halogen bond with Val A:71 (3.09 Å), a type of interaction often critical for achieving selective and stable protein-ligand complexes. In addition, the analysis indicates approximately ten van der Waals contacts, highlighting the extensive non-covalent framework that bolsters A4's positioning within the active site [46].

Among these, there are notable alkyl interactions with Val A:43 (4.80 Å) and Val A:167 (3.98 Å), as well as π-alkyl contacts with Ile A:78 (4.72 Å). The ligand also engages in π-σ\sigmaσ interactions (Thr A:165 at 3.93 Å), underscoring the tight hydrophobic packing around its aromatic moieties. These hydrophobic contacts, combined with the hydrogen-bond network and halogen interactions, confer a multidimensional stabilization of the complex; even the slightly longer π-alkyl distance of 5.25 Å with Ala A:47 highlights cooperative involvement of nearby residues in maintaining the ligand's optimal conformation.

Furthermore, three-dimensional visualization of the same binding environment integrates solvent accessibility (SAS), hydrogen-bond distribution, electrostatic charge, and hydrophobic

DOI: https://doi.org/10.17509/ajse.v6i1.89789
p- ISSN 2775-6793 e- ISSN 2775-6815

character. The SAS gradient (green to blue) delineates more buried versus more solvent-exposed regions around the ligand, while the hydrogen-bond map (magenta for donor, green for acceptor) pinpoints specific polar contacts, guiding A4's orientation toward key side-chain functionalities. The interpolated charge surface (negative in red to positive in blue) captures the electrostatic contours, unveiling areas of charge complementarity that could enhance binding affinity. Lastly, the hydrophobicity map (brown for hydrophobic to blue for hydrophilic) demonstrates the predominance of nonpolar residues in the binding pocket favorable for van der Waals interactions with A4's aromatic and aliphatic regions while small hydrophilic patches accommodate charge-dependent or hydrogen-bonding interactions [47]. Taken together, these multifaceted data provide a comprehensive view of how A4 is recognized and stabilized, showcasing the complex interplay of polar and nonpolar forces that drive ligand affinity in this protein environment.

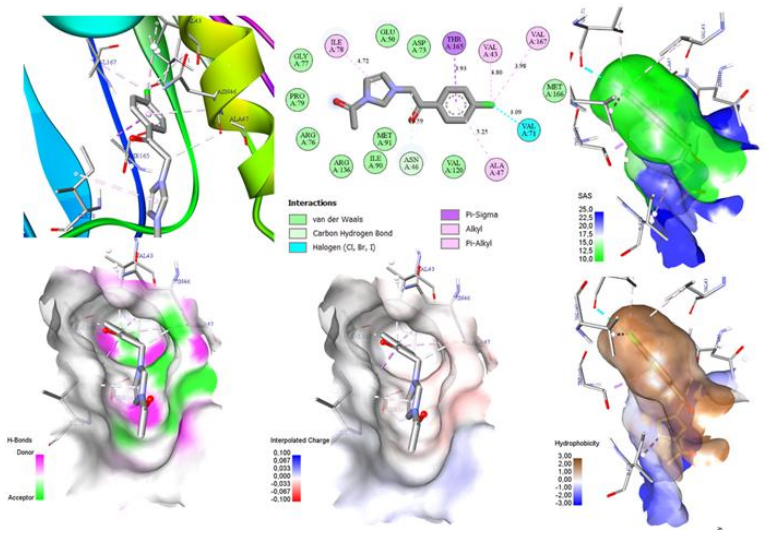

Figure 7. 2D and 3D visualizations of the docking results for ligand A4 with the E. coli protein 1KZN, highlighting key non-covalent interactions and solvent accessibility.

3.5. Molecular Dynamics Analysis: RMSD, RMSF, and Protein-Ligand Stability

Before presenting the detailed analysis of molecular dynamics, it is worth emphasizing the importance of this method for studying conformational stability and protein-ligand interactions. Indeed, molecular dynamics (MD) makes it possible to simulate the spatiotemporal evolution of a biological system (protein, ligand, solvents, etc.) under controlled thermodynamic conditions, thereby revealing structural fluctuations, the accessibility of binding pockets, and stabilization mechanisms that may not be observable in static docking models [48].

In **Figure 8**, the evolution of the RMSD (Root Mean Square Deviation) over time (horizontal axis, in nanoseconds) is shown for two entities: on the one hand, the protein backbone (red line), and on the other, the ligand A4 (black line). The red curve displays minimal fluctuation, hovering around modest values (generally below 0.3 nm), indicating that the protein maintains a globally stable structure throughout the simulation, evidence of a well-balanced system devoid of any significant unfolding. In contrast, the black curve, associated with A4, exhibits greater fluctuation: peaks can reach around 0.8 nm, indicating a more pronounced mobility of the ligand within the binding pocket.

This increase in RMSD for A4 may be explained by its chemical structure, featuring a substituted imidazolium core (e.g., a halogen group or an aromatic moiety), which confers a certain degree of conformational flexibility. Consequently, A4 can adopt various orientations,

DOI: https://doi.org/10.17509/ajse.v6i1.89789
p- ISSN 2776-6098 e- ISSN 2776-5938

form transient interactions with different key cavity residues (e.g., via hydrophobic contacts or halogen bonds), and then shift in response to local protein movements or solvent rearrangements. The fact that these RMSD values do not exceed 1 nm for prolonged periods, however, suggests that the ligand does not "escape" the site, but rather explores multiple internal positions while maintaining sufficient binding interactions to remain within the pocket.

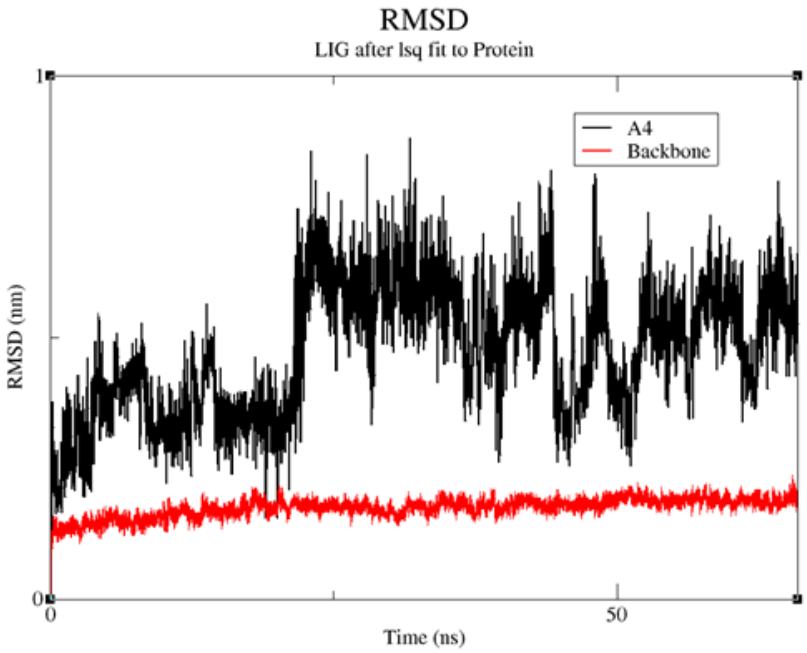

Figure 8. RMSD evolution of the protein backbone and ligand A4 during molecular dynamics simulation.

All these observations confirm the protein's stability (low backbone RMSD) and a relative freedom of movement for A4 (higher RMSD), consistent with binding modulated by the flexibility of the imidazolium skeleton and its substituents. This internal dynamic, while remaining confined to the active site, serves as an indicator of a reasonably strong affinity: the ligand does not dissociate but explores micro-conformational states that can briefly strengthen or weaken its interactions. Overall, the RMSD analysis highlights the protein's structural robustness and A4's capacity to remain associated despite noticeable fluctuations, thus corroborating the hypothesis of a stable and potentially effective interaction already suggested by the docking studies. The RMSF (Root Mean Square Fluctuation) (**Figure 9**) analysis evaluates, for each atom (or sometimes each residue) of the protein, the average amplitude of its displacements during the molecular dynamics simulation.

In the presented graph, the x-axis (from 0 to about 2800) corresponds to the index of the atoms in the protein, while the y-axis indicates the RMSF in nanometers (up to around 0.4 nm). The observation of pronounced peaks near atom indices 1000 and 1200, exceeding 0.2-0.3 nm, suggests the existence of particularly mobile regions, such as solvent-exposed loops, unstructured (or partially structured) segments, or external domains that are less sterically constrained [49]. By contrast, the portions whose fluctuation remains below 0.1 nm generally correspond to more rigid regions, such as α-helical or β-sheet cores, often buried in the protein's hydrophobic interior and contributing to the overall stability of the architecture.

DOI: https://doi.org/10.17509/ajse.v6i1.89789
p- ISSN 2775-6793 e- ISSN 2775-6815

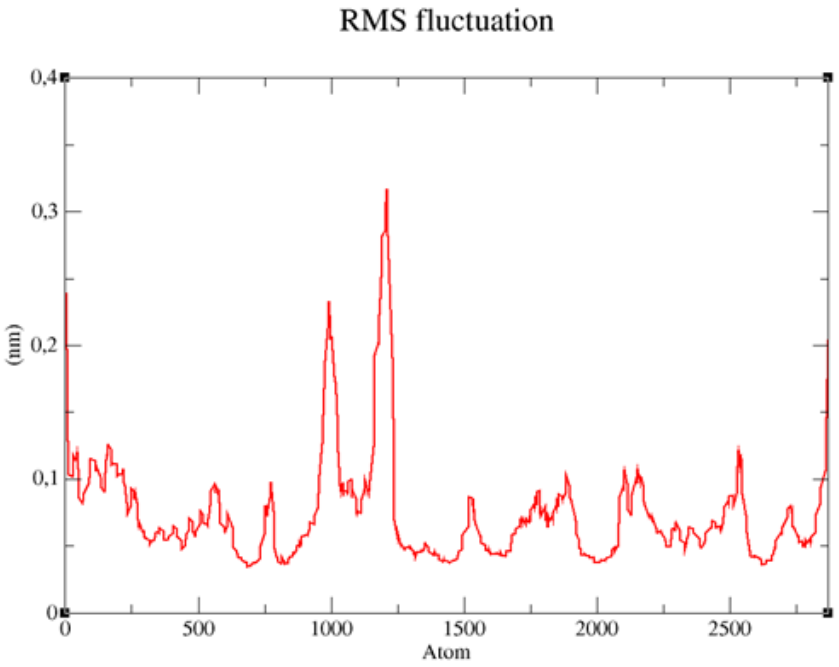

Figure 8. RMS Fluctuation of the protein backbone and ligand A4 during molecular dynamics simulation.

The presence of well-defined peaks illustrates a heterogeneous distribution of flexibility a common phenomenon in multidomain proteins or those possessing flexible structural motifs involved in ligand recognition or allosteric regulation. It is not uncommon for the N- or C-terminal ends to also exhibit high fluctuations, owing to weaker structural anchoring. In the context of studying a protein-ligand complex, this information complements the global RMSD analysis: a high RMSF can reflect local "breathing" in the protein, which may sometimes facilitate ligand access to its binding site or, conversely, alter the stability of certain key interactions. Consequently, the most prominent peaks are hypothesized to correspond to flexible regions that play a role in the protein's dynamics, potentially crucial for its biological activity. Thus, interpreting the RMSF results, combined with docking and RMSD data, provides a detailed view of conformational stability: not only is the average flexibility of the entire protein identified, but specific segments that can modulate the overall behavior of the complex through their fluctuations are also pinpointed. Finally, this study adds new information regarding molecular docking, as reported elsewhere (**Table 8**).

Table 8. Previous studies regarding molecular docking.

No	Title	Ref.
1	*Artemisia herba alba* essential oil: GC/MS analysis, antioxidant activities with molecular docking on S protein of SARS-CoV-2	[50]
2	Triazolopyrimidine derivatives: A comprehensive review of their synthesis, reactivity, biological properties, and molecular docking studies	[51]
3	Deciphering the mechanism of action *Cosmos caudatus* compounds against breast neoplasm: A combination of pharmacological networking and molecular docking approach with bibliometric analysis	[52]
4	Synthesis, antibacterial evaluation and molecular docking of 2,4,5-tri-imidazole derivatives	[53]
5	Reverse docking on five original PPO structures: Plant, bacterial, and human	[54]
6	Synthesis, optimization, DFT/TD-DFT and COX/LOX docking of new Schiff base N'-((9-ethyl-9H-carbazol-1-yl)methylene)naphthalene-2-sulfonohydrazide	[55]

DOI: https://doi.org/10.17509/ajse.v6i1.89789
p- ISSN 2776-6098 e- ISSN 2776-5938

Table 8 (Continue). Previous studies regarding molecular docking.

No	Title	Ref.
7	Synthesis, characterization, E/Z-isomerization, DFT, optical and IBNA docking of new Schiff base derived from naphthalene-2-sulfonohydrazide	[56]
8	Design, synthesis, and biological evaluation of new sulfonamides derived from 2-aminopyridine: Molecular docking, POM analysis, and identification of the pharmacophore sites	[57]
9	Computational approaches to *Spirulina platensis* growth with urea-derived nanonutrients: Thermodynamic properties, energetic profiles, molecular docking and POM analysis	[58]
10	Preparation and characterization of new mixed azo ligand complexes with some metal ions and in vitro biological activity and molecular docking study of Ni(II) and Hg(II) complexes	[59]
11	Molecular docking studies for the identifications of novel antimicrobial compounds targeting *Staphylococcus aureus*	[60]
12	Potential inhibition of ALDH by argan oil compounds, computational approach by docking, ADMET and molecular dynamics	[61]
13	3D-QSAR, molecular docking, molecular dynamic simulation, and ADMET study of bioactive compounds against *Candida albicans*	[62]
14	Acetylcholinesterase, tyrosinase, α-glucosidase inhibition of *Ammoides leucotrichus* fruits essential oil and ethanolic extract and molecular docking analysis	[63]
15	3D-QSAR modeling, molecular docking and drug-like properties investigations of novel heterocyclic compounds derived from *Magnolia officinalis* as hit compounds against NSCLC	[64]
16	Novel triazole-pyrazine as potential antibacterial agents: Synthesis, characterization, antibacterial activity, drug-likeness properties and molecular docking studies	[65]
17	Investigating the biological activities of Moroccan *Cannabis sativa* L. seed extract: Antimicrobial, anti-inflammatory, and antioxidant effects with molecular docking analysis	[66]
18	Investigation of the usability of some triazole derivative compounds as drug active ingredients by ADME and molecular docking properties	[67]
19	In silico design of new α-glucosidase inhibitors through 3D-QSAR study, molecular docking modeling and ADMET analysis	[68]
20	In search of new potent α-glucosidase inhibitors: Molecular docking and ADMET prediction	[69]
21	In silico studies of 1,4-disubstituted 1,2,3-triazole with amide functionality: Antimicrobial evaluation against *Escherichia coli* using 3D-QSAR, molecular docking, and ADMET properties	[70]
22	Deciphering the SARS-CoV-2 Delta variant: Antiviral compound efficacy by molecular docking, ADMET, and dynamics studies	[71]
23	In silico docking, drug-likeness and toxicity prediction studies of bioactive compounds of *Eurycoma longifolia* as potential multi-targeted antiviral agents against SARS-CoV-2	[72]
24	Extract and molecular docking: Exploring the oxidation of 3,5-di-tert-butylcatechol and 2-aminophenol in the presence of O_2 from air	[73]
25	Synthesis, structural and crystallographic characterization of new hydrosoluble thymol derivatives with enhanced antioxidant activity assessed by docking study	[74]
26	Synthesis, anticancer, antimicrobial evaluation, in silico molecular docking and POM analyses of new 4,7-dimethyl coumarin containing sulfonamides	[75]
27	Synthesis, spectroscopic characterization, cytotoxic activity, ADME prediction and molecular docking studies of the novel series quinoxaline-2,3-dione	[76]
28	Molecular docking and ADMET prediction of compounds from *Piper longum* L. detected by GC-MS analysis in diabetes management	[77]
29	CoMFA topomer, CoMFA, CoMSIA, HQSAR, docking molecular, dynamique study and ADMET study on phenoxypropyl isoxazole derivatives for coxsackie virus B3 inhibitors activity	[78]
30	Computational insights into benzothiophene derivatives as potential antibiotics against multidrug-resistant *Staphylococcus aureus*: QSAR modeling and molecular docking studies	[79]
31	Computational engineering of malonate and tetrazole derivatives targeting SARS-CoV-2 main protease: Pharmacokinetics, docking, and molecular dynamics insights to support the sustainable development goals (SDGs), with a bibliometric analysis	[80]

DOI: https://doi.org/10.17509/ajse.v6i1.89789
p- ISSN 2775-6793 e- ISSN 2775-6815

4. CONCLUSION

The study demonstrates that compounds A3 and A4 exhibit significant therapeutic potential, as reflected in their vigorous antibacterial activity confirmed by both in vitro assays and computational modeling. Their efficacy against E. coli and P. aeruginosa, comparable to that of gentamicin, underscores their promise as alternative antimicrobial agents. Moreover, molecular docking and molecular dynamics simulations revealed stable and favorable ligand-protein interactions, supporting their mechanistic plausibility. The compounds also displayed favorable ADMET characteristics and acceptable predicted toxicity (Class 4), further reinforcing their suitability for pharmaceutical development. However, comprehensive preclinical studies remain essential to validate their safety, efficacy, and pharmacokinetic behavior in vivo. These findings provide a compelling foundation for the continued development of imidazolium-based therapeutics targeting drug-resistant bacterial infections.

5. AUTHORS' NOTE

The authors declare that there is no conflict of interest regarding the publication of this article. Authors confirmed that the paper was free of plagiarism.

6. REFERENCES

[1] Yadav, G., and Jain, R. (2025). An insight into Synthetic, Structural and Medicinal perspective of imidazole analogs: A review. *European Journal of Medicinal Chemistry*, *290*, 117524.

[2] Martins, I. C., Al-Sabbagh, D., Meyer, K., Maiwald, M., Scholz, G., and Emmerling, F. (2019). Insight into the structure and properties of novel imidazole-based salts of salicylic acid. *Molecules*, *24*(22), 4144.

[3] Babalola, B. A., Sharma, L., Olowokere, O., Malik, M., and Folajimi, O. (2024). Advancing drug discovery: Thiadiazole derivatives as multifaceted agents in medicinal chemistry and pharmacology. *Bioorganic and Medicinal Chemistry*, *112*, 117876.

[4] Leśniewska, A., and Przybylski, P. (2024). Seven-membered N-heterocycles as approved drugs and promising leads in medicinal chemistry as well as the metal-free domino access to their scaffolds. *European Journal of Medicinal Chemistry*, *275*, 116556.

[5] Hiremath, A. F., MR, P. K., Rajagopal, K., Barua, R., Rab, S. O., Alshehri, M. A., and Emran, T. B. (2024). Imidazole-based metal complex derivatives: A comprehensive overview of synthesis and biological applications. *Medicinal Chemistry*, *21*(8), 772-807.

[6] Titi, A., Almutairi, S. M., Alrefaei, A. F., Manoharadas, S., Alqurashy, B. A., Sahu, P. K., and Ali, I. (2020). Novel phenethylimidazolium based ionic liquids: Design, microwave synthesis, in-silico, modeling and biological evaluation studies. *Journal of Molecular Liquids*, *315*, 113778.

[7] Al Johani, A. R., Almutairi, S.M., El-Sayed, W.S., Sahu, P.K., Sahu, P.K., and Messali, M. (2020). Design, sustainable synthesis, characterization, antimicrobial evaluation and in silico ADMET prediction of new functionalized imidazolium based ionic liquids. *Asian Journal of Chemistry*, *32*(8), 1972-1980.

[8] Medjahed, N., Kibou, Z., Berrichi, A., and Choukchou-Braham, N. (2023). Advances in Pyrazoles Rings' syntheses by heterogeneous catalysts, ionic liquids, and multicomponent reactions-a review. *Current Organic Chemistry*, *27*(6), 471-509.

DOI: https://doi.org/10.17509/ajse.v6i1.89789
p- ISSN 2776-6098 e- ISSN 2776-5938

[9] Zheng, X., Ma, Z., and Zhang, D. (2020). Synthesis of imidazole-based medicinal molecules utilizing the van leusen imidazole synthesis. *Pharmaceuticals*, *13*(3), 37.

[10] Abdel-Wahab, B. F., Awad, G. E., and Badria, F. A. (2011). Synthesis, antimicrobial, antioxidant, anti-hemolytic and cytotoxic evaluation of new imidazole-based heterocycles. *European Journal of Medicinal Chemistry*, *46*(5), 1505-1511.

[11] Zeng, C., Ning, Z., Xu, Y., Tian, L., Jing, J., Chen, L., and Meng, Q. (2025). The discovery of novel antimicrobial peptides against drug-resistant bacteria based on fragments fusion strategy. *European Journal of Medicinal Chemistry*, *289*, 117493.

[12] Jjemba, P. K., and Robertson, B. K. (2005). Antimicrobial agents with improved clinical efficacy versus their persistence in the environment: Synthetic 4-quinolone as an example. *EcoHealth*, *2*(3), 171-182.

[13] Bouchal, B., Abrigach, F., Takfaoui, A., Elidrissi Errahhali, M., Elidrissi Errahhali, M., Dixneuf, P. H., and Bellaoui, M. (2019). Identification of novel antifungal agents: Antimicrobial evaluation, SAR, ADME–Tox and molecular docking studies of a series of imidazole derivatives. *BMC Chemistry*, *13*(1), 100-112.

[14] Benabbou, A., Bourassi, L., Yahyaoui, M. I., Merimi, I., Challioui, A., Asehraou, A., and Siaj, M. (2024). Enhancement of bioplastic properties using metal-ligand coordination for applications in food packaging. *Interactions*, *245*(1), 292.

[15] Zhang, R., Zhang, Y., Zhang, T., Xu, M., Wang, H., Zhang, S., and Shi, G. (2022). Establishing a MALDI-TOF-TOF-MS method for rapid identification of three common Gram-positive bacteria (Bacillus cereus, Listeria monocytogenes, and Micrococcus luteus) associated with foodborne diseases. *Food Science and Technology*, *42*, e117021.

[16] Khatoon, H., and Faudzi, S. M. M. (2024). Exploring quinoxaline derivatives: An overview of a new approach to combat antimicrobial resistance. *European Journal of Medicinal Chemistry*, *276*, 116675.

[17] Gouba, N., and Drancourt, M. (2015). Digestive tract mycobiota: A source of infection. *Medecine et Maladies Infectieuses*, *45*(1-2), 9-16.

[18] Wang, X. D., Wei, W., Wang, P. F., Yi, L. C., Shi, W. K., Xie, Y. X., and Zhu, H. L. (2015). Synthesis, molecular docking and biological evaluation of 3-arylfuran-2 (5H)-ones as anti-gastric ulcer agent. *Bioorganic and Medicinal Chemistry*, *23*(15), 4860-4865.

[19] Al-Masoudi, N. A., and Abbas, Z. A. (2016). Synthesis and biological activity of new metronidazole derivatives. *Monatshefte für Chemie-Chemical Monthly*, *147*(2), 383-390.

[20] Alotaibi, B. S., Hakami, M. A., Jawaid, T., Alshammari, N., Binsuwaidan, R., and Adnan, M. (2024). Identification of potential Escherichia coli DNA gyrase B inhibitors targeting antibacterial therapy: An integrated docking and molecular dynamics simulation study. *Journal of Biomolecular Structure and Dynamics*, *42*(17), 8885-8896.

[21] Singh, R., Sindhu, J., Devi, M., Kumar, P., Lal, S., Kumar, A., and Kumar, H. (2024). Synthesis of thiazolidine-2, 4-dione tethered 1, 2, 3-triazoles as α-amylase inhibitors: in vitro approach coupled with QSAR, molecular docking, molecular dynamics and ADMET studies. *European Journal of Medicinal Chemistry*, *275*, 116623.

DOI: https://doi.org/10.17509/ajse.v6i1.89789
p- ISSN 2775-6793 e- ISSN 2775-6815

[22] Lucas, A. J., Sproston, J. L., Barton, P., and Riley, R. J. (2019). Estimating human ADME properties, pharmacokinetic parameters and likely clinical dose in drug discovery. *Expert Opinion on Drug Discovery*, *14*(12), 1313-1327.

[23] Alqahtani, S. (2017). In silico ADME-Tox Modeling: Progress and prospects. *Expert Opinion on Drug Metabolism and Toxicology*, *13*(11), 1147-1158.

[24] Jia, C. Y., Li, J. Y., Hao, G. F., and Yang, G. F. (2020). A drug-likeness toolbox facilitates ADMET study in drug discovery. *Drug discovery today*, *25*(1), 248-258.

[25] Shaabani, A., Afshari, R., Hooshmand, S. E., and Keramati Nejad, M. (2017). Molecularly imprinted polymer as an eco-compatible nanoreactor in multicomponent reactions: A remarkable synergy for expedient access to highly substituted imidazoles. *ACS Sustainable Chemistry and Engineering*, *5*(10), 9506-9516.

[26] Merimi, C., Hmada, A., Hejjaj, C., Almutairi, S. M., Lgaz, H., Messali, M., and Hammouti, B. (2024). Investigating the potency of new imidazolium ionic liquids in preventing carbon steel corrosion in acidic conditions: An integrated experimental and DFTB semi-empirical approach. *Inorganic Chemistry Communications*, *167*, 112802.

[27] Balouiri, M., Sadiki, M., and Ibnsouda, S. K. (2016). Methods for in vitro evaluating antimicrobial activity: A review. *Journal of Pharmaceutical Analysis*, *6*(2), 71-79.

[28] Jalilian, A. R., Sattari, S., Bineshmarvasti, M., Daneshtalab, M., and Shafiee, A. (2003). Synthesis and in vitro antifungal and cytotoxicity evaluation of substituted 4, 5-dihydronaphtho [1, 2-d][1, 2, 3] thia (or selena) diazoles. *Il Farmaco*, *58*(1), 63-68.

[29] Dawood, K. M., Farag, A. M., and Abdel-Aziz, H. A. (2005). Synthesis and antimicrobial evaluation of some 1, 2, 4-triazole, 1, 3, 4-oxa (thia) diazole, and 1, 2, 4-triazolo [3, 4-b]-1, 3, 4-thiadiazine derivatives. *Heteroatom Chemistry: An International Journal of Main Group Elements*, *16*(7), 621-627.

[30] Daina, A., Michielin, O., and Zoete, V. (2017). SwissADME: A free web tool to evaluate pharmacokinetics, drug-likeness and medicinal chemistry friendliness of small molecules. *Scientific Reports*, *7*(1), 42717.

[31] [33] Xiong, G., Wu, Z., Yi, J., Fu, L., Yang, Z., Hsieh, C., and Cao, D. (2021). ADMETlab 2.0: an integrated online platform for accurate and comprehensive predictions of ADMET properties. *Nucleic Acids Research*, *49*(W1), W5-W14.

[32] Mariya Kappan, M., and George, J. (2024). In Silico Pharmacokinetic and Molecular Docking Studies of Natural Plants against Essential Protein KRAS for Treatment of Pancreatic Cancer. *Journal of Natural Remedies*, *23*(3), 1107–1123.

[33] Banerjee, P., Kemmler, E., Dunkel, M., and Preissner, R. (2024). ProTox 3.0: A webserver for the prediction of toxicity of chemicals. *Nucleic Acids Research*, *52*(W1), W513-W520.

[34] Trott, O., and Olson, A. J. (2010). AutoDock Vina: improving the speed and accuracy of docking with a new scoring function, efficient optimization, and multithreading. *Journal of Computational Chemistry*, *31*(2), 455-461.

[35] Van Der Spoel D, Lindahl E, Hess B. (2005) Groenhof G, Mark AE, Berendsen HJ. GROMACS: fast, flexible, and free. J Comput Chem. 26(16), 1701–1718.

[36] Mohammed, H. H., Ali, D.M.E., Badr, M., Habib, A. G., Mahmoud, A. M., Farhan, S. M., and Abuo-Rahma, G.E.D.A. (2023). Synthesis and molecular docking of new N 4-

DOI: https://doi.org/10.17509/ajse.v6i1.89789
p- ISSN 2776-6098 e- ISSN 2776-5938

piperazinyl ciprofloxacin hybrids as antimicrobial DNA gyrase inhibitors. *Molecular Diversity*, *27*(4), 1751-1765.

[37] Veber, D. F., Johnson, S. R., Cheng, H. Y., Smith, B. R., Ward, K. W., and Kopple, K. D. (2002). Molecular properties that influence the oral bioavailability of drug candidates. *Journal of Medicinal Chemistry*, *45*(12), 2615-2623.

[38] Hammouti, Y., Elbouzidi, A., Taibi, M., Bellaouchi, R., Loukili, E. H., Bouhrim, M., and Addi, M. (2023). Screening of phytochemical, antimicrobial, and antioxidant properties of Juncus acutus from Northeastern Morocco. *Life*, *13*(11), 2135.

[39] Muhamad, N., and Na-Bangchang, K. (2023). The roles of CYP2C19 and CYP3A4 in the in vitro metabolism of β-eudesmol in human liver: Reaction phenotyping and enzyme kinetics. *Pharmacology Research and Perspectives*, *11*(6), e01149.

[40] Tetko, I. V., M. Lowe, D., and Williams, A. J. (2016). The development of models to predict melting and pyrolysis point data associated with several hundred thousand compounds mined from PATENTS. *Journal of cheminformatics*, *8*(1), 1-18.

[41] Gadaleta, D., Vuković, K., Toma, C., Lavado, G. J., Karmaus, A. L., Mansouri, K., and Roncaglioni, A. (2019). SAR and QSAR modeling of a large collection of LD50 rat acute oral toxicity data. *Journal of Cheminformatics*, *11*(1), 1-16.

[42] Rudik, A. V., Bezhentsev, V. M., Dmitriev, A. V., Druzhilovskiy, D. S., Lagunin, A. A., Filimonov, D. A., and Poroikov, V. V. (2017). MetaTox: web application for predicting structure and toxicity of xenobiotics' metabolites. *Journal of Chemical Information and Modeling*, *57*(4), 638-642.

[43] Garg, A., Saini, P., Vijeata, A., Chaudhary, G. R., Chaudhary, S., and Bhalla, A. (2025). Stereoselective synthesis and antibacterial potential of C-3 chloro β-lactams: Insights into DNA gyrase inhibition using in silico molecular docking. *International Journal of Biological Macromolecules*, *308*, 142713.

[44] [46] Rullán-Lind, C., Pietri, R. B., Vázquez-Cintrón, M., and Baerga-Ortiz, A. (2018). Fused dimerization increases expression, solubility, and activity of bacterial dehydratase enzymes. *Protein Science*, *27*(5), 969-975.

[45] Khan, S. A., Khan, S. U., Fozia, Ullah, N., Shah, M., Ullah, R., and Alotaibi, A. (2021). Isolation, structure elucidation and in silico prediction of potential drug-like flavonoids from Onosma chitralicum targeted towards functionally important proteins of drug-resistant bad bugs. *Molecules*, *26*(7), 2048.

[46] Hamami, S. M. A., Fai, M., Aththar, A. F., Zakaria, M. N. Z., Kharisma, V. D., Murtadlo, A. A. A., and Fitri, E. (2022). Nano transdermal delivery potential of fucoidan from Sargassum sp.(Brown Algae) as chemoprevention agent for breast cancer treatment. *Pharmacognosy Journal*, *14*(6), 789–795.

[47] [49] Martins, M. O., da Silva, I. Z., Fagan, S. B., and dos Santos, A. F. (2021). Docking fundamentals for simulation in nanoscience. *Disciplinarum Scientia| Naturais e Tecnológicas*, *22*(3), 67-76.

[48] [50] Ahmed, B., Khan, S., Nouroz, F., Farooq, U., and Khalid, S. (2022). Exploring multi-target inhibitors using in silico approach targeting cell cycle dysregulator–CDK proteins. *Journal of Biomolecular Structure and Dynamics*, *40*(19), 8825-8839.

DOI: https://doi.org/10.17509/ajse.v6i1.89789
p- ISSN 2775-6793 e- ISSN 2775-6815

[49] Alotaibi, B. S., Hakami, M. A., Hazazi, A., Alsaiari, A. A., Khalid, M., and Beg, A. (2024). Investigating mechanistic insights of curcumin in blocking the Interleukin-8 signaling pathway associated with Breast Cancer: An in-silico approach. *Saudi Journal of Biological Sciences*, *31*(8), 104035.

[50] Diass, K., Oualdi, I., Dalli, M., Azizi, S.E., Mohamed, M., Gseyra, N., Touzani, R., and Hammouti, B. (2023). Artemisia herba alba essential oil: GC/MS analysis, antioxidant activities with molecular docking on S protein of SARS-CoV-2. *Indonesian Journal of Science and Technology*, *8*(1), 1-18.

[51] El Mrayej, H., En-Nabety, G., Ettahiri, W., Jghaoui, M., Sabbahi, R., Hammouti, B., Rais, Z. and Taleb, M. (2025). Triazolopyrimidine derivatives: A comprehensive review of their synthesis, reactivity, biological properties, and molecular docking studies. *Indonesian Journal of Science and Technology*, *10*(1), 41-74.

[52] Hendrarti, W., Umar, A. H., Syahruni, R., Rafi, M., and Kusuma, W. A. (2024). Deciphering the mechanism of action cosmos caudatus compounds against breast neoplasm: A combination of pharmacological networking and molecular docking approach with bibliometric analysis. *Indonesian Journal of Science and Technology*, *9*(2), 527-556.

[53] Abbas, S. K., Jaafar, M. T., Ali, H. R., and Alsarayreh, A. A. (2024). Synthesis, Antibacterial Evaluation and molecular docking of 2,4,5-Tri-imidazole Derivatives. *Moroccan Journal of Chemistry*, *12*(3), 1222-1239.

[54] Abdessadak, O., Hajji, H., Mehanned, S., Ajana, M. A., Lakhlifi, T., and Bouachrine, M. (2022). Reverse docking on five original PPO structures: Plant, bacterial, and human. *Moroccan Journal of Chemistry*, *10*(3), 442-451.

[55] Abu-Rayyan, A., Shalalin, K., Suleiman, M., Warad, I., and Sawatfa, A. (2024). Synthesis, optimization, DFT/TD-DFT and COX/LOX docking of new Schiff base N'-((9-ethyl-9H-carbazol-1-yl) methylene) naphthalene-2-sulfonohydrazide. *Moroccan Journal of Chemistry,* 12(1), 78–88.

[56] Abu-Rayyan, A., Suleiman, M., Daraghmeh, A., Sawatfa, A., and Warad, I. (2023). Abu-Rayyan, A., Suleiman, M., Daraghmeh, A., Al Ali, A., Zarrouk, A., Kumara, K., and Warad, I. (2023). Synthesis, characterization, E/Z-isomerization, DFT, optical and 1BNA docking of new Schiff base derived from naphthalene-2-sulfonohydrazide. *Moroccan Journal of Chemistry*, *11*(3), 613–622.

[57] Ahamed, L.S., Sallal, Z.A., Al-Jelaiwi, O.H.R., Shamaya, A.N.S., and Mahmood, A.A.R. (2025). Design, synthesis, and biological evaluation of new sulfonamides derived from 2-aminopyridine: Molecular docking, POM analysis, and identification of the pharmacophore sites. *Moroccan Journal of Chemistry*, *13*(2), 519–539.

[58] Ainane, A., Abdoul-Latif, F. M., Achenani, L., Ben Hadda, T., and Ainane, T. (2025). Computational approaches to Spirulina platensis growth with urea-derived nanonutrients: Thermodynamic properties, energetic profiles, molecular docking and POM analysis of pharmacophore sites. *Moroccan Journal of Chemistry*, *13*(3), 1210–1227.

[59] Ali, F. J., Radhi, E. R., Kadhium, A. J., and Ali, K. J. (2023). Preparation and characterization of new mixed azo ligand complexes with some metal ions and in vitro biological activity and molecular docking study of their Ni(II) and Hg(II) complexes. *Moroccan Journal of Chemistry*, *11*(4), 965–978.

DOI: https://doi.org/10.17509/ajse.v6i1.89789
p- ISSN 2776-6098 e- ISSN 2776-5938

[60] Aoumer, N., Tchouar, N., Belaidi, S., Lanez, T., and Chitta, S. (2021). Molecular docking studies for the identifications of novel antimicrobial compounds targeting Staphylococcus aureus. *Moroccan Journal of Chemistry*, *9*(2), 274–289.

[61] Bekkouch, A., Mostafi, H. E., Merzouki, M., Challouqi, A., and Mesfioui, A. (2024). Potential inhibition of ALDH by argan oil compounds, computational approach by docking, ADMET and molecular dynamics. *Moroccan Journal of Chemistry*, *12*(2), 676–695.

[62] Bouamrane, S., Khaldan, A., Hajji, H., Bouachrine, M., and Lakhlifi, T. (2022). 3D-QSAR, molecular docking, molecular dynamic simulation, and ADMET study of bioactive compounds against Candida albicans. *Moroccan Journal of Chemistry*, *10*(3), 523–541.

[63] Boumezzourh, A., Ouknin, M., Merzouki, M., Umoren, S. A., and Majidi, L. (2023). Acetylcholinesterase, tyrosinase, α-glucosidase inhibition of Ammoides leucotrichus Coss. & Dur. fruits essential oil and ethanolic extract and molecular docking analysis. *Moroccan Journal of Chemistry*, *11*(4), 1287–1298.

[64] Daoui, O., El Mouhi, R., Barghady, F., Elkhaldi, R., and Benjelloun, A. T. (2022). 3D-QSAR modeling, molecular docking and drug-like properties investigations of novel heterocyclic compounds derived from Magnolia officinalis as hit compounds against NSCLC. *Moroccan Journal of Chemistry*, *10*(4), 881–890.

[65] Filali, M., Lahyaoui, M., Bahsis, L., Kandri Rodi, Y., and El-Hadrami, E. M. (2024). Novel triazole-pyrazine as potential antibacterial agents: Synthesis, characterization, antibacterial activity, drug-likeness properties and molecular docking studies. *Moroccan Journal of Chemistry*, 13(2), 1367–1379.

[66] Haddou, S., Mounime, K., Loukili, E. H., Hammouti, B., and Chahine, A. (2023). Investigating the biological activities of Moroccan Cannabis sativa L. seed extract: Antimicrobial, anti-inflammatory, and antioxidant effects with molecular docking analysis. *Moroccan Journal of Chemistry*, *11*(4), 1116–1136.

[67] İslamoğlu, E., and Hacfazlıoğlu, E. (2022). Investigation of the usability of some triazole derivative compounds as drug active ingredients by ADME and molecular docking properties. *Moroccan Journal of Chemistry*, *10*(4), 861–880.

[68] Khaldan, A., Bouamrane, S., El-Mernissi, R., Bouachrine, M., and Lakhlifi, T. (2022). In silico design of new α-glucosidase inhibitors through 3D-QSAR study, molecular docking modeling and ADMET analysis. *Moroccan Journal of Chemistry*, *10*(1), 22–36.

[69] Khaldan, A., Bouamrane, S., El-Mernissi, R., Lakhlifi, T., and Sbai, A. (2022). In search of new potent α-glucosidase inhibitors: Molecular docking and ADMET prediction. *Moroccan Journal of Chemistry*, *10*(4), 772–786.

[70] Koubi, Y., Hajji, H., Moukhliss, Y., Bouachrine, M., and Lakhlifi, T. (2022). In silico studies of 1,4-disubstituted 1,2,3-triazole with amide functionality: Antimicrobial evaluation against Escherichia coli using 3D-QSAR, molecular docking, and ADMET properties. *Moroccan Journal of Chemistry*, *10*(4), 689–702.

[71] Merzouki, M., Bourassi, L., Abidi, R., Sabbahi, R., and Challouqi, A. (2024). Deciphering the SARS-CoV-2 Delta variant: Antiviral compound efficacy by molecular docking, ADMET, and dynamics studies. *Moroccan Journal of Chemistry*, *12*(3), 1153–1171.

DOI: https://doi.org/10.17509/ajse.v6i1.89789
p- ISSN 2775-6793 e- ISSN 2775-6815

[72] Ravichandran, V., Raghuraman, S., Prabha, T., Harish, R., and Parasuraman, P. (2025). In silico docking, drug-likeness and toxicity prediction studies of bioactive compounds of Eurycoma longifolia as potential multi-targeted antiviral agents against SARS-CoV-2. *Moroccan Journal of Chemistry*, *13*(1), 381–404.

[73] Riouchi, O., Bouroumane, N., Boutaybi, M. E., Bouyanzer, A., and Touzani, R. (2025). Extract and molecular docking: Exploring the oxidation of 3,5-di-tert-butylcatechol and 2-aminophenol in the presence of O_2 from air: Towards valuable organic compounds. *Moroccan Journal of Chemistry*, *13*(1), 145–167.

[74] Sabour, A., Elsabhani, A., Maymoun, G., Kazzaoui, S. E., and El-Maimouni, L. (2024). Synthesis, structural and crystallographic characterization of new hydrosoluble thymol derivatives with enhanced antioxidant activity assessed by docking study. *Moroccan Journal of Chemistry*, *12*(3), 554–569.

[75] Safi, M. N., Ahamed, L. S., Almalki, F. A., and Hadda, T. B. (2025). Synthesis, anticancer, antimicrobial evaluation, in silico molecular docking and POM analyses of new 4,7-dimethyl coumarin containing sulfonamides. *Moroccan Journal of Chemistry*, *13*(2), 849–880.

[76] Seggat, Y., Hafez, B., Lahyaoui, M., Chahdi, F. O., and Sebbar, N. K. (2024). Synthesis, spectroscopic characterization, cytotoxic activity, ADME prediction and molecular docking studies of the novel series quinoxaline-2,3-dione. *Moroccan Journal of Chemistry*, *13*(3), 1323–1349.

[77] Shrestha, R. L. S., Panta, R., Maharjan, B., Marasini, B. P., and Subin, J. A. (2024). Molecular docking and ADMET prediction of compounds from Piper longum L. detected by GC-MS analysis in diabetes management. *Moroccan Journal of Chemistry, 12*(2), 776–798.

[78] Tabti, K., El Mchichi, L., Moukhliss, Y., Bouachrine, M., and Lakhlifi, T. (2022). CoMFA topomer, CoMFA, CoMSIA, HQSAR, docking molecular, dynamique study and ADMET study on phenoxypropyl isoxazole derivatives for coxsackie virus B3 virus inhibitors activity. *Moroccan Journal of Chemistry*, *10*(4), 703–725.

[79] Yaqoubi, M. E., Hafez, B., Lahyaoui, M., Rodi, Y. K., and Sebbar, N. K. (2025). Computational insights into benzothiophene derivatives as potential antibiotics against multidrug-resistant Staphylococcus aureus: QSAR modeling and molecular docking studies. *Moroccan Journal of Chemistry*, *12*(2), 774–806.

[80] Merzouki, M., Khibech, O., Fraj, E., Bouammali, H., Bourhou, C., Hammouti, B., Bouammali, B., and Challioui, A. (2025). Computational engineering of malonate and tetrazole derivatives targeting SARS-CoV-2 main protease: Pharmacokinetics, docking, and molecular dynamics insights to support the sustainable development goals (SDGs), with a bibliometric analysis. *Indonesian Journal of Science and Technology*, *10*(2), 399-418.

DOI: https://doi.org/10.17509/ajse.v6i1.89789
p- ISSN 2776-6098 e- ISSN 2776-5938